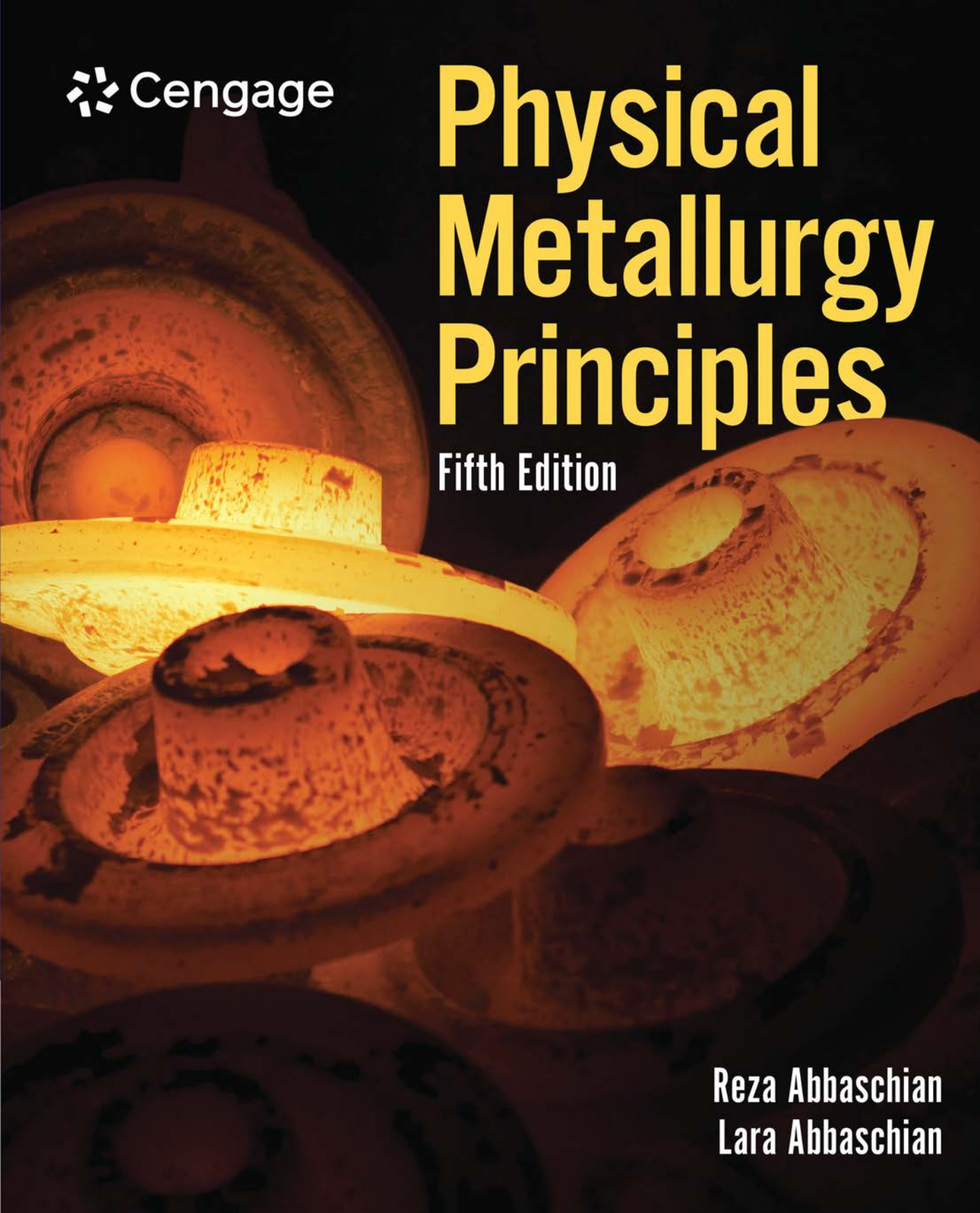
Cengage
Physical Metallurgy Principles
Fifth Edition
Reza Abbaschian
Lara Abbaschian

Physical Metallurgy Principles

Fifth Edition

Physical Metallurgy Principles

Fifth Edition

Reza Abbaschian
Lara Abbaschian

Cengage

Australia • Brazil • Canada • Mexico • Singapore • United Kingdom • United States

***Physical Metallurgy Principles*, Fifth Edition**

Reza Abbaschian, Lara Abbaschian

SVP, Product: Cheryl Costantini

VP, Product: Thais Alencar

Portfolio Product Director: Rita Lombard

Senior Portfolio Product Manager: Timothy Anderson

Product Assistant: Emily Smith

Learning Designer: MariCarmen Constable

Content Manager: Samantha Enders

Digital Project Manager: Nikkita Kendrick

VP, Product Marketing: Jason Sakos

Senior Director, Product Marketing: Danae April

Product Marketing Manager: Mackenzie Paine

Content Acquisition Analyst: Deanna Ettinger

Production Service: MPS Limited, RPK Editorial Services

Designer: Chris Doughman

Cover Image Source: Jackfoto/ Shutterstock.com

Library of Congress Control Number: 2024931732

ISBN: 979-8-214-00166-1

Cengage
5191 Natorp Boulevard
Mason, OH 45040
USA

Cengage is a leading provider of customized learning solutions. Our employees reside in nearly 40 different countries and serve digital learners in 165 countries around the world. Find your local representative at **www.cengage.com.**

To learn more about Cengage platforms and services, register or access your online learning solution, or purchase materials for your course, visit **www.cengage.com.**

Printed in the United States of America
Print Number: 01 Print Year: 2024

Dedication

We dedicate this edition in honor of Professor Robert E. Reed-Hill,
who spent a lifetime to advance physical metallurgy.
We also give special thanks to Janette, Cyrus, Gwen, David and Emily.

Contents

Chapter 4 Introduction to Dislocations 86

Chapter 5 Dislocations and Plastic Deformation 123

Chapter 8 Annealing 223

Chapter 9 Solid Solutions 267

Chapter 18 The Iron-Carbon Alloy System 576

Chapter 19 The Hardening of Steel 618

Preface

The original philosophy of the text has been preserved in this Fifth Edition. The theoretical approach to physical metallurgy is premised on the belief that the properties of metals and alloys are determined by simple physical laws. The conceptional framework used throughout is based on the fundamentals of the materials structure-properties-processing-performance relationships. As such, it is not necessary to consider each alloy as a separate entity nor to spend time learning large numbers of apparently unrelated facts that are easily forgotten. Today's alloys and methods have evolved since the publication of the First Edition and will continue to do so. However, the approach embodied by this text ensures a foundational understanding that translates into durable utility and relevance.

We have retained the easy-to-read format so that the essence of the information is most successfully communicated. Throughout the years, we have found this format to be very useful not only to current students, but also to practitioners who would like to refresh their knowledge of the field of physical metallurgy principles.

This book is intended for use as a comprehensive introduction to metallurgy and materials science and engineering. It is appropriate for all engineering students at the junior or senior level. Graduate students seeking to engage with the materials structure-properties-processing-performance relationship as they develop their research plans will also find the book valuable. Recommended prerequisites to this text are college physics, chemistry, and strength of materials. An engineering course in thermodynamics or physical chemistry is also considered desirable, but not essential since relevant core concepts are explained in Chapters 7, 10, and 11. When this textbook is used for a one semester course, a number of chapters dealing with advanced topics, such as Chapters 10, 11, and 15, may be omitted. Alternatively, the newly added Learning Objectives can serve as a guide for topic selection and syllabus creation.

Features of the Book

Following the theme of this text's pedagogy, properties-processing and performance as well as the strong interrelationship among them are discussed in the early chapters. Chapters 1 through 3 cover the structure of metals, characterization, and bonding of atoms, in that order. Because of the importance of sophisticated techniques that reach atomic-level resolution, Chapter 2 covers x-ray techniques, scanning electron microscopy, transmission and scanning transmission electron microscopy, as well as Auger electron spectroscopy. Chapters 4 and 5 cover geometrical aspects of dislocations, slip planes, and directions during plastic deformation, followed by Chapter 6 with discussion of grain boundaries and their important effects on mechanical behavior. Chapter 7 introduces a broad coverage of thermodynamic concepts, vacancies, their motion, and interstitial impurity atoms. Chapter 8 introduces annealing of cold-worked metals, recrystallization, and the release of stored energy of deformation. Chapters 9 through 11 provide background information on solid solutions, phases, and phase diagrams, which form the foundations for alloy development. Chapters 12 and 13 deal with substitutional and interstitial diffusion and kinetic concepts. Chapters 14 and 15 cover liquid-solid and solid-solid phase transformation, microstructural developments

and compositions, and growth kinetics. Theories of precipitation hardening and development of precipitates during aging of Al-Cu alloys are covered in Chapter 16. Twinning and martensitic transformations are discussed in Chapter 17, together with phenomenological crystallographic theory of martensite formation followed by its reversibility in shape-memory alloys. Chapter 18 presents an in-depth look at isothermal transformations of austenite to pearlite or bainite, their microstructures and kinetics, and the TTT diagrams of eutectoid and non-eutectoid steels. In Chapter 19, martensite formation during continuous cooling is explained with a specific focus on atomic rearrangement, hardenability, influence of composition, and grain size. The last half of the chapter discusses tempering and the effect of temperature and time on physical properties. Chapter 20 covers the important topic of non-ferrous metals. In the final chapter, Chapter 21, failure of metals and alloys is covered including cleavage, brittle and ductile failures, and fatigue.

New to This Edition

The subject matter of *Physical Metallurgy Principles* is fundamental and borne out of decades of research by pioneers that does not disappear at the introduction of this Fifth Edition. Recent references have been incorporated to complement the remaining original references, which provide historic context. Indeed, with today's electronic search engines limited to more recently published literature, such identification and acknowledgment of the pioneers of the field often get overlooked. Other changes introduced in the Fifth Edition are the addition of chapter-by-chapter Learning Objectives to improve learning outcomes, new figures to augment understanding of the text, and the inclusion of color and enhancement to figures to increase usability.

Acknowledgments

The authors would like to acknowledge the critical inputs and contributions of all who are listed in the prefaces of the earlier editions. Our gratitude extends to A. S. Nowick, W. D. Robertson, F. N. Rhines, Richard W. Heckel, Walter S. Owen, Marvin Metzger, John Kronsbein, John Hren, Robert T. DeHoff, Derek Dove, Ellis Verink, William C. Leslie, Daniel N. Beshers, Paul C. Holloway, Rolf N. Hummel, William A. Jesser, William G. Ovens, Dale E. Wittmer, James C. M. Li, Alan R. Pelton, Samuel J. Hruska, Richard B. Griffin, Dong-Joo (Daniel) Kim, Anthony P. Reynolds, Christopher A. Schuh, Jiahong Zhu, Abraham Munitz, and Gerald Bourne. Special thanks to the publishing team for this edition: Tim Anderson, Samantha Enders, Rose Kernan, and John Kronsbein. We also thank Shahin Amini and Steven Herrera for contributing some pictures incorporated in this edition.

Last, and most important, we would like to acknowledge that this text would not exist were it not for the late Professor Reed-Hill and his vision of a comprehensive tome dedicated to the field of metallurgy and materials science. One of the authors (R.A.) remembers many hours of intellectually stimulating discussions with Professor Reed-Hill and other colleagues at the University of Florida.

Reza Abbaschian
Lara Abbaschian

About the Authors

Reza Abbaschian

Reza Abbaschian is Director of Winston Chung Global Energy Center, Distinguished Professor, and Winston Chung Endowed Professor in Sustainability at University of California Riverside (UCR). He began his tenure at UCR in September 2005 as Dean of the Bourns College of Engineering (BCOE), a position that he held until July 2016. Prior to his appointment as dean at UCR, Dr. Abbaschian was the Vladimir A. Grodsky Professor of Materials Science and Engineering Department at the University of Florida, where he also served as Chair of the Department for 16 years. During his tenure, the Department rose to a *U.S. News & World Report* top-ten ranking for both undergraduate and graduate education.

Dr. Abbaschian received his PhD in Materials Science and Engineering from the University of California, Berkeley, his MS in Metallurgical Engineering from Michigan Technological University, and his BSc in Mining and Metallurgy from Tehran University. He has published more than 250 scientific articles including eight books on subjects ranging from metal processing to composites and high temperature-high pressure growth of diamonds. His research led to the introduction of man-made diamonds to the market by Gemesis Diamond Company and he holds five patents and eight trade secrets held by Gemesis.

Dr. Abbaschian is a past President of ASM International. His awards include the TMS Educator Award, Structural Material Division's Distinguished Scientist/Engineer Award, TMS Leadership Award, ASEE Donald E. Marlowe Award, Davis Productivity Award of the State of Florida, and the ASM Albert Sauveur Achievement Award. He has been elected a Fellow of ASM, TMS, and AAAS. In 2017, he was bestowed the AIME Honorary Membership, an honor bestowed on only 1/10th of 1% of its membership, in recognition of being an "outstanding scientist and researcher in solidification fundamentals and materials processing, educator and leader in advancing the materials profession."

Lara Abbaschian

Lara Abbaschian received her M.Eng. and S.B. degrees in Materials Science and Engineering from Massachusetts Institute of Technology. As a graduate student at MIT, Lara was a member of the Langer Lab, a Whitaker Fellow, and a recipient of the John Wulff Award for Excellence in Teaching. Lara holds an MBA from the Tuck School of Business at Dartmouth where she was a Forté Fellow. In her professional capacity, Lara has been awarded the Pinnacle Award and the Brain Award.

Lara has built her career at the forefront of medical device and materials innovation beyond the university setting. Her professional experience encompasses more than 20 years in the multidisciplinary healthcare space across a range of therapeutic areas and cutting-edge technologies, including cardiovascular implants, neurovascular interventional devices, stents, drug-device interfaces, and novel materials platforms. Lara has contributed to all facets of the medical device lifecycle—from inception through commercialization. Her deep experience involves bridging research and early-stage innovation to real-world realization in the highly regulated industry of medical technology. Her expertise in company venture funding and formation, product strategy and growth, and in-house R&D have allowed her to bring numerous life-saving technologies from early ideation to market and into the hands of clinicians.

Digital Resources

MindTap Reader

Available via our digital subscription service, Cengage Unlimited, **MindTap Reader** is Cengage's next-generation eBook for engineering students.

The MindTap Reader provides more than just text learning for the student. It offers a variety of tools to help our future engineers learn chapter concepts in a way that resonates with their workflow and learning styles.

- **Personalize their experience**

Within the MindTap Reader, students can highlight key concepts, add notes, and bookmark pages. These are collected in My Notes, ensuring they will have their own study guide when it comes time to study for exams.

- **Flexibility at their fingertips**

The ReadSpeaker feature reads text aloud to students, so they can learn on the go—wherever they are.

Cengage Read

Available on iOS and Android smartphones, the MindTap Mobile App provides convenience. Students can access their entire textbook anyplace and anytime. They can take notes, highlight important passages, and have their text read aloud whether they are online or off.

To download the mobile app, visit https://www.cengage.com/mindtap/mobileapp.

Cengage Unlimited

All-You-Can-Learn Access with Cengage Unlimited

Cengage Unlimited is the first-of-its-kind digital subscription that gives students total and on-demand access to all the digital learning platforms, eBooks, online homework, and study tools Cengage has to offer—in one place, for one price. With Cengage Unlimited, students get access to their WebAssign courseware, as well as content in other Cengage platforms and course areas from day one. That's 70 disciplines and 675 courses worth of material, including engineering.

With Cengage Unlimited, students get **unlimited access** to a library of more than 22,000 products. To learn more, visit https://www.cengage.com/unlimited.

Chapter 1

The Structure of Metals

Learning Objectives

Upon completion of Chapter 1, you will be able to:

1. Describe, via examples, how the structure of a material impacts its properties and, thus, its applications
2. Define the difference between microstructure and macrostructure
3. Draw the unit cell structure for face-centered cubic, body-centered cubic, and hexagonal close-packed lattices
4. Diagram how planes of atoms come together to form close-packed structures
5. Explain coordination numbers, anisotropy, and how manufacturing processes can impact both
6. Create Miller indices for crystallographic directions and crystallographic planes
7. Use a stereographic projection to map three-dimensional structure in two dimensions
8. Understand the use of Wulff nets to identify planes, directions and poles

The most important aspect of any engineering material is its structure, because its properties are closely related to this feature. To be successful, a materials engineer must have a good understanding of this relationship between structure and properties. By way of illustration, wood is a very easy material in which to see the close interaction between structure and properties. A typical structural wood, such as southern yellow pine, is essentially an array of long hollow cells or fibers. These fibers, which are formed largely from cellulose, are aligned with the grain of the wood and are cemented together by another weaker organic material called lignin. The structure of wood is thus roughly analogous to that of a bundle of drinking straws. It can be split easily along its grain; that is, parallel to the cells. Wood is also much stronger in compression (or tension) parallel to its grain than it is in compression (or tension) perpendicular to the grain. It makes excellent columns and beams, but it is not really suitable for tension members required to carry large loads, because the low resistance of wood to shear parallel to its grain makes it difficult to attach end fastenings that will not pull out. As a result, wooden bridges and other large wooden structures are often constructed containing steel tie rods to support the tensile loads.

1.1 The Structure of Metals

The structure in metals is of similar importance to that in wood, although often in a more subtle manner. Metals are usually crystalline when in the solid form. A *crystal* is defined as an orderly array of atoms in space. While very large single crystals can be prepared, the normal metallic object consists of an aggregate of many very small crystals. Metals are therefore *polycrystalline*. The crystals in these materials are normally referred to as its grains. Because of their very small sizes, an optical microscope, operating at magnifications between about 100 and 1000 times, is usually used to examine the structural features associated with the grains in a metal. Structures requiring this range of magnification for their examination fall into the class known as *microstructures*. Occasionally, metallic objects, such as castings, may have very large crystals that are discernible to the naked eye or are easily resolved under a low-power microscope. Structure in this category is called *macrostructure*. On the other hand, there are materials whose grains or sizes are much finer and in the nanoscale range. These microstructures are commonly referred to as nanostructure, with scales on the order of one billionth of a meter. It should be noted that nanoscale features can be in one dimension, as in nanosurfaces or nanofilms; in two dimensions, as in nanotubes or whiskers; or in three dimensions, as in nanoparticles. Nanoprecipitates such as Guinier and Preston (GP) Zones have been used for decades for precipitation hardening of aluminum alloys, as discussed in Chapter 16. Finally, there is the basic structure inside the grains themselves: that is, the atomic arrangements inside the crystals. This form of structure is logically called the *crystal structure*.

Of the various forms of structure, microstructure (that visible under the optical microscope) has been historically of the greatest use and interest to the metallurgist. Because the metallurgical microscope is normally operated at magnifications where its depth of field is extremely shallow, the metallic surface to be observed must be very flat. At the same time, it must reveal accurately the nature of the structure inside the metal. One is therefore presented with the problem of preparing a very smooth flat and undistorted surface, which is by no means an easy task. The procedures required to obtain the desired goal fall under the general heading of metallographic specimen preparation. Examination of the polished surface is often aided by slight chemical attacking of the surface, called "etching." During etching, grain boundaries and certain orientations are attacked more than others. Detailed description of metallographic sample preparation techniques and examples of microstructures can be found in Reference 1.

There are many different types of crystal structures, some of which are quite complicated. Fortunately, most metals crystallize in one of three relatively simple structures: the face-centered cubic, the body-centered cubic, and the close-packed hexagonal.

1.2 Unit Cells

The *unit cell* of a crystal structure is the smallest group of atoms possessing the symmetry of the crystal which, when repeated in all directions, will develop the crystal lattice. Figure 1.1A shows the unit cell of the body-centered cubic lattice. It is evident that its name is derived from the shape of the unit cell. Eight unit cells are combined in Fig. 1.1B in order to show how the unit cell fits into the complete lattice. Note that atom *a* of Fig. 1.1B does not belong uniquely to one

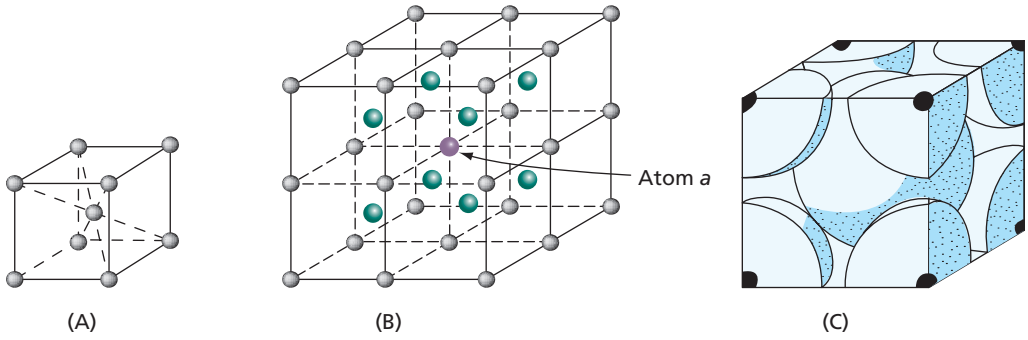

Fig. 1.1 **(A)** Body-centered cubic unit cell. **(B)** Eight unit cells of the body centered cubic lattice. **(C)** Cut view of a unit cell. The coloring scheme is used for ease of visuallization. Otherwise all atoms are the same.

unit cell, but is a part of all eight unit cells that surround it. Therefore, it can be said that only one-eighth of this corner atom belongs to any one-unit cell. This fact may be used to compute the number of atoms per unit cell in a body-centered cubic crystal. Even a small crystal will contain billions of unit cells, and the cells in the interior of the crystal must greatly exceed in number than those lying on the surface. Therefore, surface cells may be neglected in our computations. In the interior of a crystal, each corner atom of a unit cell is equivalent to atom *a* of Fig. 1.1B and contributes one-eighth of an atom to a unit cell. In addition, each cell also possesses an atom located at its center that is not shared with other unit cells. The body-centered cubic lattice thus has two atoms per unit cell; one contributed by the corner atoms, and one located at the center of the cell, as shown in Fig. 1.1C.

The unit cell of the face-centered cubic lattice is shown in Fig. 1.2. In this case, the unit cell has an atom in the center of each face. The number of atoms per unit cell in the face-centered cubic lattice can be computed in the same manner as in the body-centered cubic lattice. The eight corner atoms again contribute one atom to the cell, as shown in Fig. 1.2B. There are also six face-centered

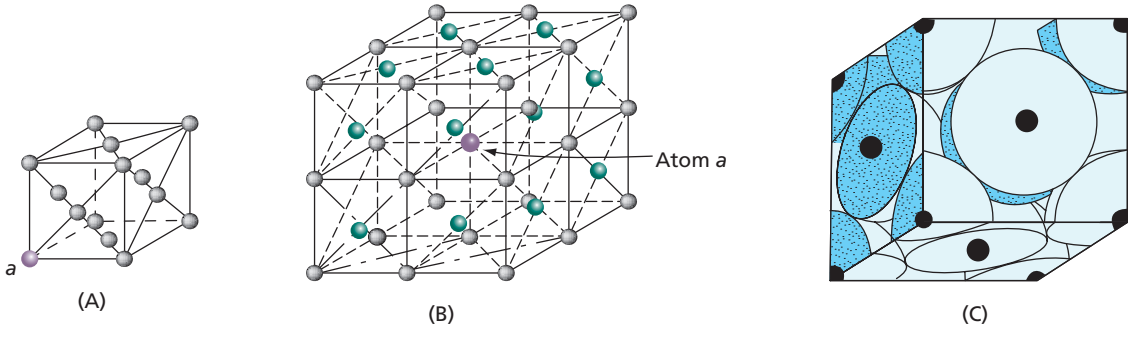

Fig. 1.2 **(A)** Face-centered cubic unit cell. **(B)** Eight unit cells of the face-centered cubic lattice. The face-centered atoms of the top, front and right side faces are shown. **(C)** Cut view of a unit cell

atoms to be considered, each a part of two unit cells. These contribute six times one-half an atom, or three atoms. The face-centered cubic lattice has a total of four atoms per unit cell, or twice as many as the body-centered cubic lattice.

1.3 The Body-Centered Cubic Structure (BCC)

It is frequently convenient to consider metal crystals as structures formed by stacking together hard spheres. This leads to the so-called *hard-ball model* of a crystalline lattice, where the radius of the spheres is taken as half the distance between the centers of the most closely spaced atoms.

Figure 1.3 shows the hard-ball model of the body-centered cubic (bcc) unit cell. A study of the figure shows that the atom at the center of the cube is colinear with each corner atom; that is, the atoms connecting diagonally opposite corners of the cube form straight lines, each atom touching the next in sequence. These linear arrays do not end at the corners of the unit cell, but continue on through the crystal much like a row of beads strung on a wire (see Fig. 1.1B). These four cube diagonals constitute the close-packed directions of the body-centered cubic crystal, directions that run continuously through the lattice on which the atoms are as closely spaced as possible.

Further consideration of Figs. 1.3 and 1.1B reveals that all atoms in the body-centered cubic lattice are equivalent. Thus, the atom at the center of the cube of Fig. 1.3 has no special significance over those occupying corner positions. Each of the latter could have been chosen as the center of a unit cell, making all corner atoms of Fig. 1.1B centers of cells, and all centers of cells corners.

1.4 Coordination Number of the Body-Centered Cubic Lattice

The coordination number (CN) of a crystal structure equals the number of nearest neighbors that an atom possesses in the lattice. In the body-centered cubic unit cell, the center atom has eight neighbors touching it (see Fig. 1.3). We have already seen that all atoms in this lattice

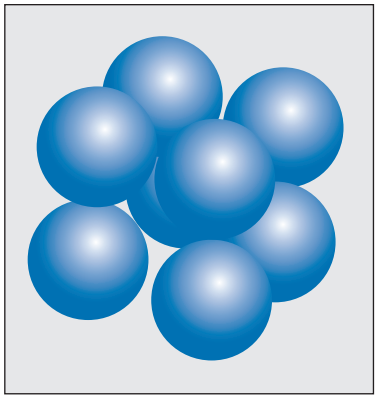

Fig. 1.3 Hard-ball model of the body-centered cubic unit cell

are equivalent. Therefore, every atom of the body-centered cubic structure not lying at the exterior surface possesses eight nearest neighbors, and the coordination number of the lattice is eight.

1.5 The Face-Centered Cubic Lattice (FCC)

The hard-ball model assumes special significance in the face-centered cubic crystal, for in this structure the atoms or spheres are packed together as closely as possible. The CN for fcc is 12. Figure 1.4A shows a complete face-centered cubic (fcc) cell, and Fig. 1.4B shows the same unit cell with a corner atom removed to reveal a close-packed plane (octahedral plane) in which the atoms are spaced as tightly as possible. A larger area from one of these close-packed planes is shown in Fig. 1.5. Three close-packed directions lie in the octahedral plane (the directions *aa, bb*, and *cc*). Along these directions the spheres touch and are colinear.

Returning to Fig. 1.4A, we see that the close-packed directions of Fig. 1.5 correspond to diagonals that cross the faces of the cube. There are six of these close-packed directions in the face-centered cubic lattice, as shown in Fig. 1.4C. Face diagonals lying on the reverse faces of the cube are not counted in this total because each is parallel to a direction lying on a visible face, and, in considering crystallographically significant directions, parallel directions are the same. It should also be pointed out that the face-centered cubic structure has four close-packed or octahedral planes. This can be verified as follows. If an atom is removed from each of the corners of a unit cell in a manner similar to that of Fig. 1.4B, an octahedral plane will be revealed in each instance. There are eight of these planes, but since diagonally opposite planes are parallel, they are crystallographically equal. This reduces the number of different octahedral planes to four. The face-centered cubic lattice, however, is unique in that it contains as many as four planes of closest packing, each containing three close-packed directions. No other lattice possesses such a large number of close-packed planes and closed-packed directions. This fact is important, since it gives face-centered cubic metals physical properties different from those of other metals, one of which is the ability to undergo severe plastic deformation.

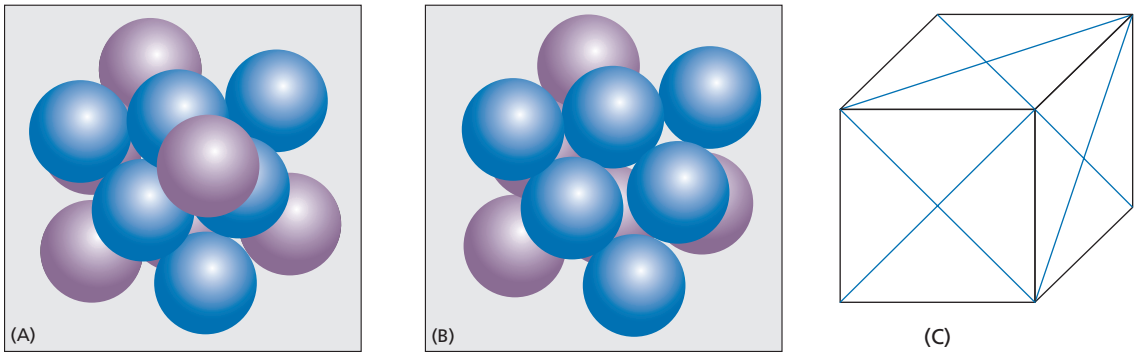

Fig. 1.4 **(A)** Face-centered cubic unit cell (hard-ball model). **(B)** Same cell with a corner atom removed to show an octahedral plane. **(C)** The six-face diagonal directions

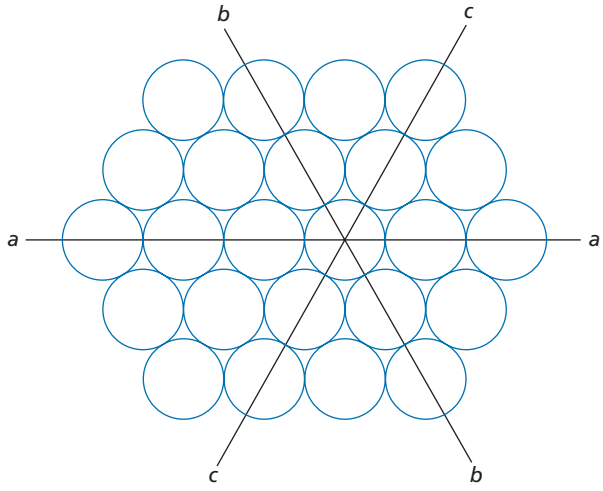

Fig. 1.5 Atomic arrangement in the octahedral plane of a face-centered cubic metal. Notice that the atoms have the closest possible packing. This same configuration of atoms is also observed in the basal plane of close-packed hexagonal crystals. The close-packed directions are *aa*, *bb*, and *cc*

1.6 The Unit Cell of the Hexagonal Closed-Packed (HCP) Lattice

The configuration of atoms most frequently used to represent the hexagonal close-packed structure is shown in Fig. 1.6. This group of atoms contains more than the minimum number of atoms needed to form an elementary building block for the lattice; therefore it is not a true unit cell. However, because the arrangement of Fig. 1.6, which contains three primitive cells, brings out important crystallographic features, including the sixfold symmetry of the lattice, it is commonly used as the unit cell of the close-packed hexagonal structure. A comparison of Fig. 1.6 with Fig. 1.5 shows that the atoms in the planes at the top, bottom, and center of the unit cell belong to a plane of closest packing, the basal plane of the crystal. The figure also shows that the atoms in these basal planes have the proper stacking sequence for the hexagonal close-packed lattice (*ABA* . . .); atoms at the top of the cell are directly over those at the bottom, while atoms in the central plane have a different set of positions.

The basal plane of a hexagonal metal, like the octahedral plane of a face-centered cubic metal, has three close-packed directions. These directions correspond to the lines *aa, bb, cc* of Fig. 1.5.

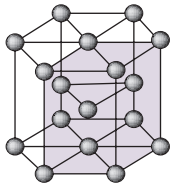

Fig. 1.6 The close-packed hexagonal unit cell

1.7 Comparison of the Face-Centered Cubic and Close-Packed Hexagonal Structures

The face-centered cubic lattice can be constructed by first arranging atoms into a number of close-packed planes, similar to that shown in Fig. 1.5, and then by stacking these planes over each other in the proper sequence. There are a number of ways in which planes of closest packing can be stacked. One sequence gives the close-packed hexagonal lattice, another the face-centered cubic lattice. The reason that there is more than one way of stacking close-packed planes is because any one plane can be set down on a previous one in two different ways. For example, consider the close-packed plane of atoms in Fig. 1.7. The center of each atom in the figure is indicated by the symbol A. Now, if a single atom is placed on top of the configuration of Fig. 1.7, it will be attracted by interatomic forces into one of the natural pockets that occur between any three contiguous atoms. Suppose that it falls into the pocket marked B_1 at the upper left of the figure; then a second atom cannot be dropped into either C_1 or C_2 because the atom at B_1 overlaps the pocket at these two points. However, the second atom can fall into B_2 or B_3 and start the formation of a second close-packed plane consisting of atoms occupying all B positions. Alternatively, the second plane could have been set down in such a way as to fill only C positions. Thus if the first close-packed plane occupies A positions, the second plane may occupy B or C positions. Let us assume that the second plane has the B configuration. Then the pockets of the second plane fall half over the centers of the atoms in the first plane (A positions) and half over the C pockets in the first plane. The third plane may now be set down over the second plane into either A or C positions. If set down into A positions, the atoms in the third layer fall directly over atoms in the first layer. This is not the face-centered cubic order, but that of the close-packed hexagonal structure. The face-centered cubic stacking order is: A for the first plane, B for the second plane, and C for the third plane, which may be written as ABC. The fourth plane in the face-centered cubic lattice, however, does fall on the A position, the fifth on B, and the sixth on C, so that the stacking order for face-centered cubic crystals is $ABCABCABC$, etc. In the close-packed hexagonal structure, the atoms in every other plane fall directly over one another, corresponding to the stacking order $ABABAB\ldots$.

There is no basic difference in the packing obtained by the stacking of spheres in the face-centered cubic or the close-packed hexagonal arrangement, since both give an ideal close-packed structure. There is, however, a marked difference between the physical properties of hexagonal close-packed metals (such as cadmium, zinc, and magnesium) and the face-centered

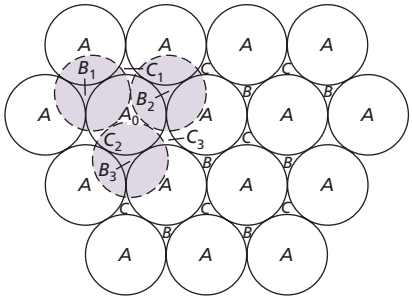

Fig. 1.7 Stacking sequences in close-packed crystal structures

cubic metals, (such as aluminum, copper, and nickel), which is related directly to the difference in their crystalline structure. The most striking difference is in the number of close-packed planes. In the face-centered cubic lattice there are four planes of closest packing, the *octahedral planes*; but in the close-packed hexagonal lattice only one plane, the *basal plane*, is equivalent to the octahedral plane. The single close-packed plane of the hexagonal lattice engenders, among other things, plastic deformation properties that are much more directional than those found in cubic crystals.

1.8 Coordination Number of the Systems of Closest Packing

The *coordination number* of an atom in a crystal has been defined as the number of nearest neighbors that it possesses. This number is 12 for both face-centered cubic and close-packed hexagonal crystals, as may be verified with the aid of Fig. 1.7. Thus, consider atom A_0 lying in the plane of atoms shown as circles drawn with continuous lines. Six other atoms lying in the same close-packed plane as A_0 are in nearest neighbor positions. Atom A_0 also touches three atoms in the plane directly above. These three atoms could occupy B positions, as is indicated by the dashed lines around pockets B_1, B_2, and B_3, or they could occupy positions C_1, C_2, and C_3. In either case, the number of nearest neighbors in the plane just above A_0 is limited to three. In the same manner, it may be shown that A_0 has three nearest neighbors in the next plane below the close-packed plane containing A_0. The number of nearest neighbors of atom A_0 is thus twelve: six in its own plane, three in the plane above it, and three in the plane below it. Since the argument is valid no matter whether the atoms in the close-packed planes just above or below atom A_0 are in B or C positions, it holds for both face-centered cubic and close-packed hexagonal stacking sequences. We conclude, therefore, that the coordination number in these lattices is 12.

1.9 Anisotropy

When the properties of a substance are independent of direction, the material is said to be isotropic. Thus, in an isotropic material, one should expect to find that it has the same strength in all directions. Or, if its electrical resistivity were measured, the same value of this property would be obtained irrespective of how a resistivity specimen was cut from a quantity of the material. The physical properties of crystals normally depend strongly on the direction along which they are measured. This means that, basically, crystals are not isotropic, but anisotropic. In this regard, consider a body-centered cubic crystal of iron. The three most important directions in this crystal are the directions labeled *a, b*, and *c* in Fig. 1.8. That these directions are not equivalent can be recognized from the fact that the spacings of the atoms along the three directions are different, being equal respectively, in terms of the lattice parameter a (the length of one edge of the unit cell), to a, $\sqrt{2a}$, and $\sqrt{\frac{3}{2}a}$. The physical properties of iron, measured along these three directions, also tend to be different. As an example, consider the *I-H* curve for the magnetization of iron crystals. As may be seen in Fig. 1.9, the intensity of magnetization I rises most rapidly with the magnetic field intensity H along the direction a, at an intermediate rate along b, and least rapidly along c. Interpreted in another way, we may say that a is the direction of easiest magnetization, while c is correspondingly the most difficult. Another example is shown for nickel single crystals. Here the intensity of magnetization rises rapidly in the direction c and least rapidly in direction a.

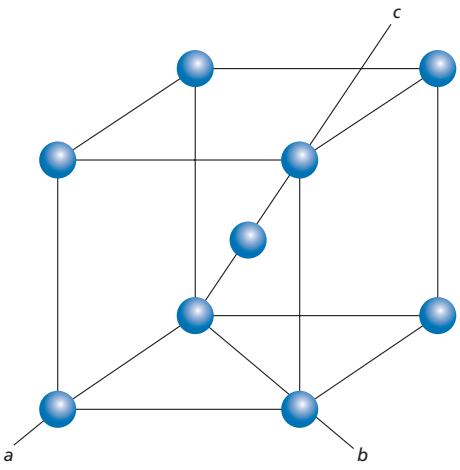

Fig. 1.8 The most important directions in a body-centered cubic crystal

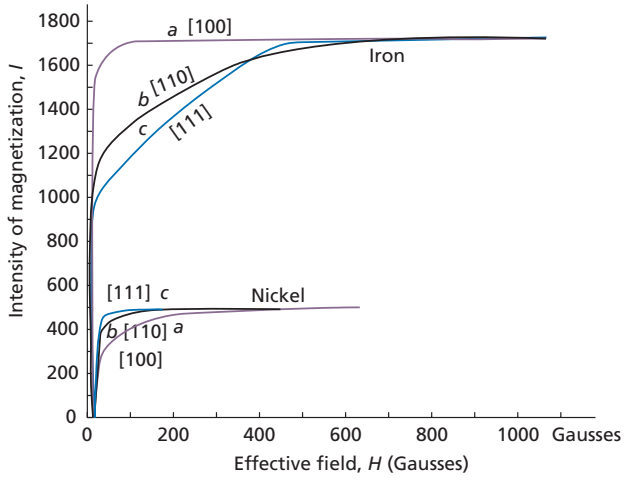

Fig. 1.9 An iron crystal is much easier to magnetize along an *a* direction of Fig. 1.8 than along a *b* or *c* direction. The opposite is the case for nickel (Refs. 2 and 3)

It should be noted that the above-mentioned bulk anisotropies relate to the crystal structures. When these materials are used in thin layers having a thickness on the order of a few atomic layers, additional anistropies related to surfaces and interfaces may also appear (Ref. 4).

Ideally, a polycrystalline specimen might be expected to be isotropic if its crystals were randomly oriented, for then, from a macroscopic point of view, the anisotropy of the crystals should be averaged out. However, a truly random arrangement of the crystals is seldom achieved, because manufacturing processes tend to align the grains in a metal so that their orientations are not uniformly distributed. The result is known as a texture or a preferred orientation. Because most polycrystalline metals have a preferred orientation, they tend to be anisotropic, the degree of this anisotropy depending on the degree of crystal alignment.

1.10 Textures or Preferred Orientations

Wires are formed by pulling rods through successively smaller and smaller dies. In the case of iron, this kind of deformation tends to align a *b* direction of each crystal parallel to the wire axis. About this direction the crystals are normally considered to be randomly arranged. This type of preferred arrangement of the crystals in an iron or steel wire is quite persistent. Even if the metal is given a heat treatment* that completely reforms the crystal structure, the crystals tend to keep a *b* direction parallel to the wire axis. Because the deformation used in forming sheets and plates is basically two-dimensional in character, the preferred orientation found in them is more restrictive than that observed in wires. As indicated in Fig. 1.10A, not only does one tend to find a *b* direction parallel

*Recrystallization following cold work is discussed in Chapter 8.

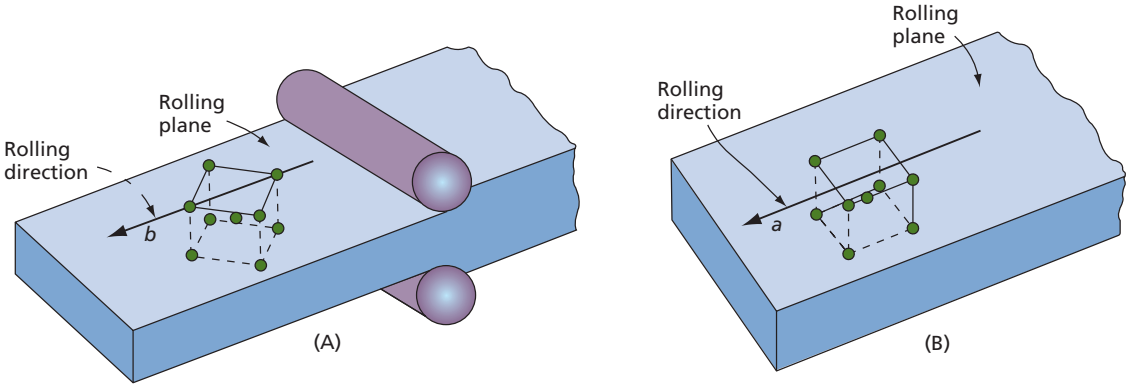

Fig. 1.10 Two basic crystalline orientations that can be obtained in rolled plates of body-centered cubic metals

to the rolling direction or length of the plate, but there is also a strong tendency for a cube plane, or face of the unit cell, to be aligned parallel to the rolling plane or surface of the sheet or plate.

There are a number of reasons why an understanding of crystal properties is important to engineers. One of these is that the basic anisotropy of crystalline materials is reflected in the polycrystalline objects of commerce. It should be noted also that this is not always undesirable. Preferred orientations can often result in materials with superior properties. An interesting example of this sort is found in the alloy of iron with 4 percent of silicon, used for making transformer coils. In this case, by a complicated combination of rolling procedures and heat treatments, it is possible to obtain a very strong preferred orientation in which an *a* direction of the crystals is aligned parallel to the rolling direction, while a cube plane, or face of the unit cell, remains parallel to the rolling plane. This average orientation is shown schematically in Fig. 1.10B. The significant feature of this texture is that it place the direction of easy magnetization parallel to the length of the sheet. In manufacturing transformers, it is then a rather simple matter to align the plates in the core so that this direction is parallel to the direction along which the magnetic flux runs. When this occurs, the resultant hysteresis loss can be made very small.

1.11 Miller Indices

As one becomes more and more involved in the study of crystals, the need for symbols to describe the orientation in space of important crystallographic directions and planes becomes evident. Thus, while the directions of closest packing in the body-entered cubic lattice may be described as the diagonals that traverse the unit cell, and the corresponding directions in the face-centered cubic lattice as the diagonals that cross the faces of a cube, it is much easier to define these directions in terms of several simple integers. The Miller system of designating indices for crystallographic planes and directions is universally accepted for this purpose. In the discussion that follows, the Miller indices for cubic and hexagonal crystals will be considered. The indices for other crystal structures are not difficult to develop.

Direction Indices in the Cubic Lattice Let us take a cartesian coordinate system with axes parallel to the edge of the unit cell of a cubic crystal. (See Fig. 1.11.) In this coordinate system, the unit of measurement along all three axes is the length of the edge of a unit cell, designated by the symbol a in the figure. The Miller indices of directions are introduced with the aid of several simple examples. Thus the cube diagonal m of Fig. 1.11 has the same direction as a vector t with a length that equals the diagonal distance across the cell. The component of the vector t on each of the three coordinate axes is equal to a. Since the unit of measurement along each axis equals a, the vector has components 1, 1 and 1 on the x, y, and z axes, respectively. The Miller indices of the direction m are now written [111]. In the same manner, the direction n, which crosses a face of the unit cell diagonally, has the same direction as a vector s the length of which is the face diagonal of the unit cell. The x, y, and z components of this vector are 1, 0 and 1 respectively; the corresponding Miller indices are [101]. The indices of the x axis are [100], the y axis [010], and the z axis [001].

A general rule for finding the Miller indices of a crystallographic direction can now be stated. Draw a vector from the origin parallel to the direction whose indices are desired. Make the magnitude of the vector such that its components on the three coordinate axes have lengths that are simple integers. These integers must be the smallest numbers that will give the desired direction. Thus, the integers 1, 1, and 1, and 2, 2, and 2 represent the same direction in space, but, by convention, the Miller indices are [111] and not [222].

Let us apply the above rule to the determination of the Miller indices of a second cube diagonal; that indicated by the symbol p in Fig. 1.12. The vector (which starts at the origin in Fig. 1.12B) is parallel to the direction p. The components of q are 1, −1, and 1, and, by the above definition, the corresponding Miller indices of p are $[1\bar{1}1]$, where the negative sign of the y index is indicated by a bar over the corresponding integer. The indices of the diagonal m in Fig. 1.12A have already been shown to be [111], and it may also be shown that the indices of the diagonals u and v are $[11\bar{1}]$ and $[\bar{1}11]$. The four cube diagonals thus have indices [111], $[\bar{1}11]$, $[1\bar{1}1]$, and $[11\bar{1}]$.

When a specific crystallographic direction is referred to, the Miller indices are enclosed in square brackets as shown here. However, it is sometimes desirable to refer to all of the directions of the same form. In this case, the indices of one of these directions are enclosed in carets ⟨111⟩, and the symbol is read to signify all four directions ([111], $[\bar{1}11]$, $[1\bar{1}1]$, and $[11\bar{1}]$), which are considered as a class. Thus, one might say that the close-packed directions in the body-centered cubic lattice are ⟨111⟩ directions, whereas a specific crystal might be stressed in tension along its [111] direction and simultaneously compressed along its $[1\bar{1}1]$ direction.

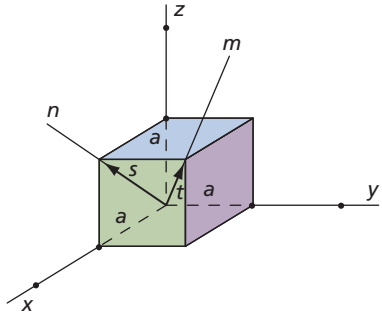

Fig. 1.11 The [111] and [101] directions in a cubic crystal; directions m and n, respectively

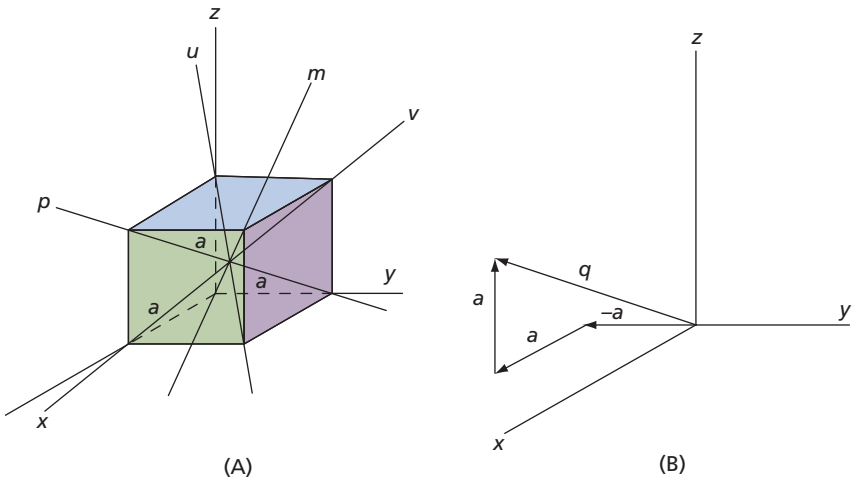

Fig. 1.12 **(A)** The four cube diagonals of a cubic lattice, *m, n, u,* and *v*. **(B)** The components of the vector *q* that parallels the cube diagonal *p* are *a, −a,* and *a*. Therefore, the indices of *q* are [111]

Cubic Indices for Planes Crystallographic planes are also identified by sets of integers. These are obtained from the intercepts that the planes make with the coordinate axes. Thus, in Fig. 1.13 the indicated plane intercepts the *x, y*, and *z* axes at 1, 3, and 2 unit-cell distances, respectively. The Miller indices are proportional not to these intercepts, but to their reciprocals $\frac{1}{1}, \frac{1}{3}, \frac{1}{2}$ and, by definition, the Miller indices are the smallest integers having the same ratios as these reciprocals. The desired integers are, therefore, 6, 2, 3. The Miller indices of a plane are enclosed in parentheses, for example (623), instead of brackets, thus making it possible to differentiate between planes and directions.

Let us now determine the Miller indices of several important planes of cubic crystals. The plane of the face *a* of the cube shown in Fig. 1.14A is parallel to both the *y* and *z* axes and, therefore, may be said to intercept these axes at infinity. The *x* intercept, however, equals 1, and the reciprocals of the three intercepts are $\frac{1}{1}, \frac{1}{\infty}, \frac{1}{\infty}$. The corresponding Miller indices are (100). The indices of the face *b* are (010), while those of *c* are (001). The indicated plane of Fig. 1.14B has indices (011), and that of Fig. 1.14C (111). The latter plane is an octahedral plane, as may be seen by referring

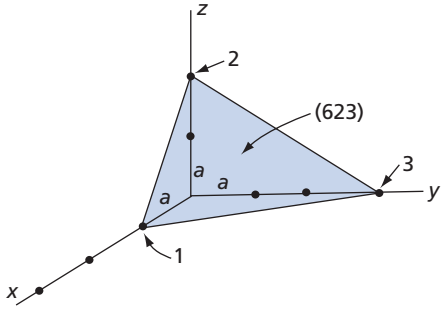

Fig. 1.13 The intercepts of the (623) plane with the coordinate axes

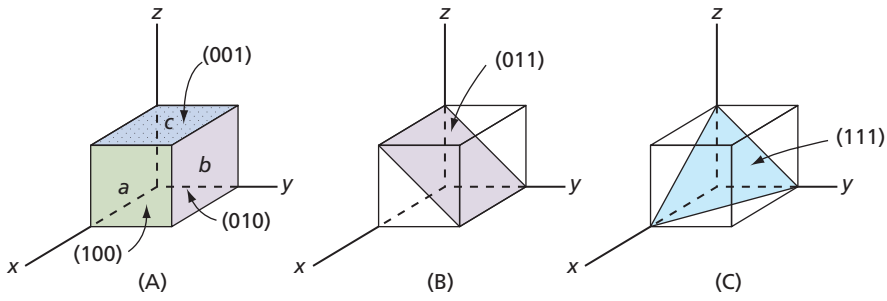

Fig. 1.14 **(A)** Cube planes of a cubic crystal: *a* (100); *b* (010); *c* (001). **(B)** The (011) plane. **(C)** The (111) plane

to Fig. 1.15. Other octahedral planes have the indices $(\bar{1}11)$, $(1\bar{1}1)$, and $(11\bar{1})$, where the bar over a digit represents a negative intercept. By way of illustration, the $(\bar{1}11)$ plane is shown in Fig. 1.15, where it may be seen that the *x* intercept is negative, whereas the *y* and *z* intercepts are positive. This figure also shows that the $(1\,\bar{1}\,\bar{1})$ plane is parallel to the $(\bar{1}11)$ plane and is, therefore, the same crystallographic plane. Similarly, the indices $(\bar{1}1\bar{1})$ and $(\bar{1}\,\bar{1}1)$ represent the same planes as $(1\bar{1}1)$ and $(11\bar{1})$, respectively.

The set of planes of a given form, such as the four octahedral planes (111), $(1\bar{1}1)$, $(\bar{1}11)$, and $(11\bar{1})$, are represented as a group with the aid of braces enclosing one of the indices, that is, {111}. Thus, if one wishes to refer to a specific plane in a crystal of known orientation, parentheses are used, but if the class of planes is to be referred to, braces are used.

An important feature of the Miller indices of cubic crystals is that the integers of the indices of a plane and of the direction normal to the plane are identical. Thus, face *a* of the cube in Fig. 1.14A has indices (100), and the *x* axis, perpendicular to this plane, has indices [100]. In the same manner, the octahedral plane of Fig. 1.14C and its normal, the cube diagonal, have indices (111) and [111], respectively. Noncubic crystals do not, in general, possess this equivalence between the indices of planes and normals to the planes. The spacing between crystallographic planes is covered later in Section 2.4.

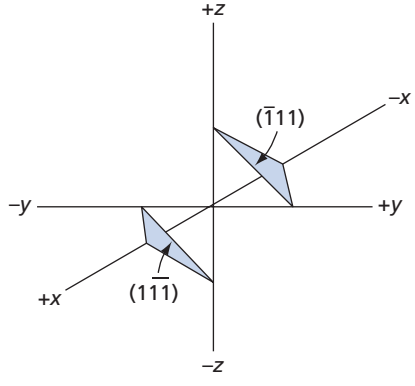

Fig. 1.15 The $(\bar{1}11)$ and $(1\,\bar{1}\,\bar{1})$ planes are parallel to each other and therefore represent the same crystallographic plane

Miller Indices for Hexagonal Crystals Planes and directions in hexagonal metals are defined almost universally in terms of Miller indices containing four digits instead of three. The use of a four-digit system gives planes of the same form similar indices. Thus, in a four-digit system, the planes $(11\bar{2}0)$ and $(1\bar{2}10)$ are equivalent planes. The three-digit system, on the other hand, gives equivalent planes indices that are not similar. Thus, the previously mentioned two planes would have indices (110) and $(1\bar{2}0)$ in the three-digit system.

Four-digit hexagonal indices are based on a coordinate system containing four axes. Three axes correspond to close-packed directions and lie in the basal plane of the crystal, making 120° angles with each other. The fourth axis is normal to the basal plane and is called the c axis, where as the three axes that lie in the basal plane are designated the a_1, a_2, and a_3 axes. Figure 1.16 shows the hexagonal unit cell superimposed upon the four-axis coordinate system. It is customary to take the unit of measurement along the a_1, a_2, and a_3 axes as the distance between atoms in a close-packed direction. The magnitude of this unit is indicated by the symbol a. The unit of measurement for the c axis is the height of the unit cell that is designated as c.

Let us now determine the Miller indices of several important close-packed hexagonal lattice planes. The uppermost surface of the unit cell in Fig. 1.16 corresponds to the basal plane of the crystal. Since it is parallel to the axes a_1, a_2, and a_3, it must intercept them at infinity. Its c axis intercept, however, is equal to 1. The reciprocals of these intercepts are $\frac{1}{\infty}, \frac{1}{\infty}, \frac{1}{\infty}, \frac{1}{1}$. The Miller indices of the basal plane are, therefore, (0001). The six vertical surfaces of the unit cell are known as *prism planes* of Type 1. Consider now the prism plane that forms the front face of the cell, which has intercepts as follows: a_1 at 1, a_2 at ∞, a_3 at -1, and c at ∞. Its Miller indices are, therefore, $(10\bar{1}0)$. Another important type of plane in the hexagonal lattice is shown in Fig. 1.17. The intercepts are a_1 at 1, a_2 at ∞, a_3 at -1, and c at $\frac{1}{2}$, and the Miller indices are accordingly $(10\bar{1}2)$.

Miller indices of directions are also expressed in terms of four digits. In writing direction indices, the third digit must always equal the negative sum of the first two digits. Thus, if the first two digits are 3 and 1, the third must be -4, that is, $[31\bar{4}0]$.

Let us investigate directions lying only in the basal plane, since this will simplify the presentation. If a direction lies in the basal plane, then it has no component along the c axis, and the fourth digit of the Miller indices will be zero.

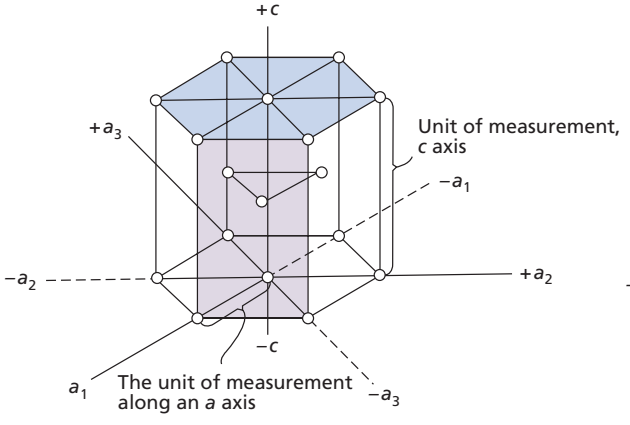

Fig. 1.16 The four coordinate axes of a hexagonal crystal

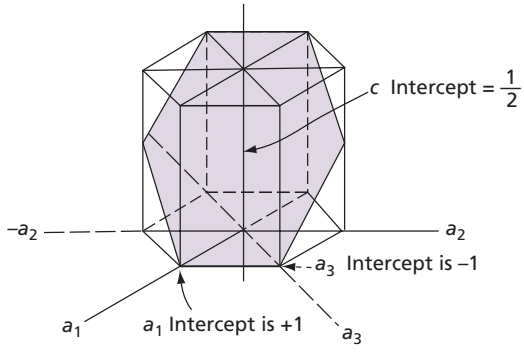

Fig. 1.17 The $(10\bar{1}2)$ plane of a hexagonal metal

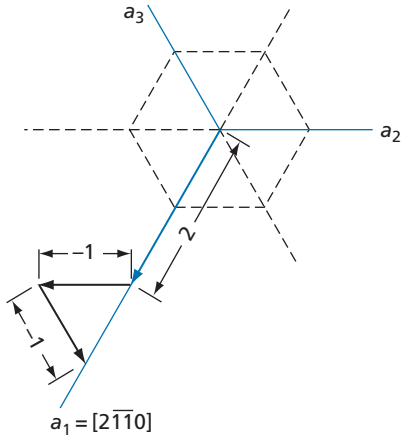

Fig. 1.18 Determination of indices of a digonal axis of Type I—$[2\bar{1}\bar{1}0]$

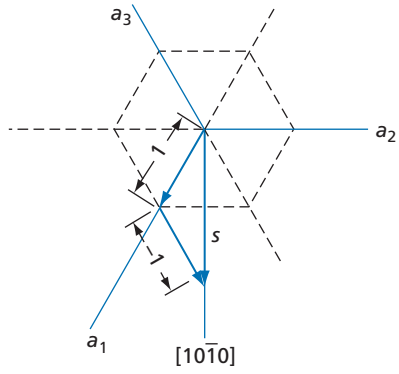

Fig. 1.19 Determination of indices of a digonal axis of Type II—$[10\bar{1}0]$

As our first example, let us find the Miller indices of the a_1 axis. This axis has the same direction as the vector sum of three vectors (Fig. 1.18), one of length +2 along the a_1 axis, another of length −1 parallel to the a_2 axis, and the third of length −1 parallel to the a_3 axis. The indices of this direction are, accordingly $[2\bar{1}\bar{1}0]$. This unwieldy method of obtaining the direction indices is necessary in order that the relationship mentioned above be maintained between the first two digits and the third. The corresponding indices of the a_2 and a_3 axes are $[\bar{1}2\bar{1}0]$ and $[\bar{1}\bar{1}20]$. These three directions are known as the digonal axes of Type I. Another important set of directions lying in the basal plane are the digonal axes of Type II; a set of axes perpendicular to the digonal axes of Type I. Figure 1.19 shows one of the axes of Type II and indicates how its direction indices are determined. The vector s in the figure determines the desired direction and equals the vector sum of a unit vector lying on a_1, and another parallel to a_3, but measured in a negative sense. The indices of the digonal axis of Type II are thus $[10\bar{1}0]$. In this case, the second digit is zero because the projection of the vector s on the a_2 axis is zero.

1.12 Crystal Structures of the Metallic Elements

Crystalline structures can form in two-dimensional or three-dimensional space. A good example of the former is graphene, which is a single layer of carbon atoms arranged in a hexagonal lattice, with each atom tightly bonded to three other carbon atoms. A review of graphene, its properties, and applications can be found in a recent review by Urade et al. (Ref. 5). In three-dimensional space, atoms can be arranged in seven lattice systems, consisting of Cubic, Hexagonal, Tetragonal, Orthorhombic, Rhombohedral, Monoclinic and Triclinic (Ref. 6). These primitive unit cells may also contain additional atoms as body-centered, face-centered, or base-centered lattices, leading to total of 14 lattice systems often referred to as Bravais lattices.

Some of the most important metals are classified according to their crystal structures in Table 1.1.

Table 1.1 Crystal Structure of Some of the More Important Metallic Elements

Face-Centered Cubic	Closed-Packed Hexagonal	Body-Centered Cubic
Iron (911.5 to 1396 °C)	Magnesium	Iron (below 911.5 and from 1396 to 1538 °C)
Copper	Zinc	Titanium (882 to 1670 °C)
Silver	Titanium (below 882 °C)	Zirconium (863 to 1855 °C)
Gold	Zirconium (below 863 °C)	Tungsten
Aluminum	Beryllium	Vanadium
Nickel	Cadmium	Molybdenum
Lead		Alkali Metals (Li, Na, K, Rb, Ca)
Platinum		

A number of metals are polymorphic, that is, they crystallize in more than one structure. The most important of these is iron, which crystallizes as either body-centered cubic or face-centered cubic, with each structure stable in separate temperature ranges. Thus, at all temperatures below 911.5 °C and above 1396 °C to the melting point, the preferred crystal structure is body-centered cubic, whereas between 911.5 °C and 1396 °C the metal is stable in the face-centered cubic structure. It may also be seen in Table 1.1 that titanium and zirconium are also polymorphic, being body-centered cubic at higher temperatures and close-packed hexagonal at lower temperatures.

1.13 The Stereographic Projection

The stereographic projection is a useful metallurgical tool, for it permits the mapping in two dimensions of crystallographic planes and directions in a convenient and straightforward manner.* The real value of the method is attained when it is possible to visualize crystallographic features directly in terms of their stereographic projections. The purpose of this section is to concentrate on the geometrical correspondence between crystallographic planes and directions and their stereographic projections. In each case, a sketch of a certain crystallographic feature, in terms of its location in the unit cell, is compared with its corresponding stereographic projection.

Several simple examples will be considered, but before this is done, attention will be called to several pertinent facts. The stereographic projection is a two-dimensional drawing of three-dimensional data. The geometry of all crystallographic planes and directions is accordingly reduced by one dimension. Planes are plotted as great circle lines, and directions are plotted as points. Also, the normal to a plane completely describes the orientation of a plane.

As our first example, consider several of the more important planes of a cubic lattice: specifically the (100), (110), and (111) planes. All three planes are treated in the three parts of Fig. 1.20. Notice that the stereographic projection of each plane can be represented either by a great circle or by a point showing the direction in space that is normal to the plane.

*Stereographic projection is used for analysis of diffraction patterns discussed in Chapter 2.

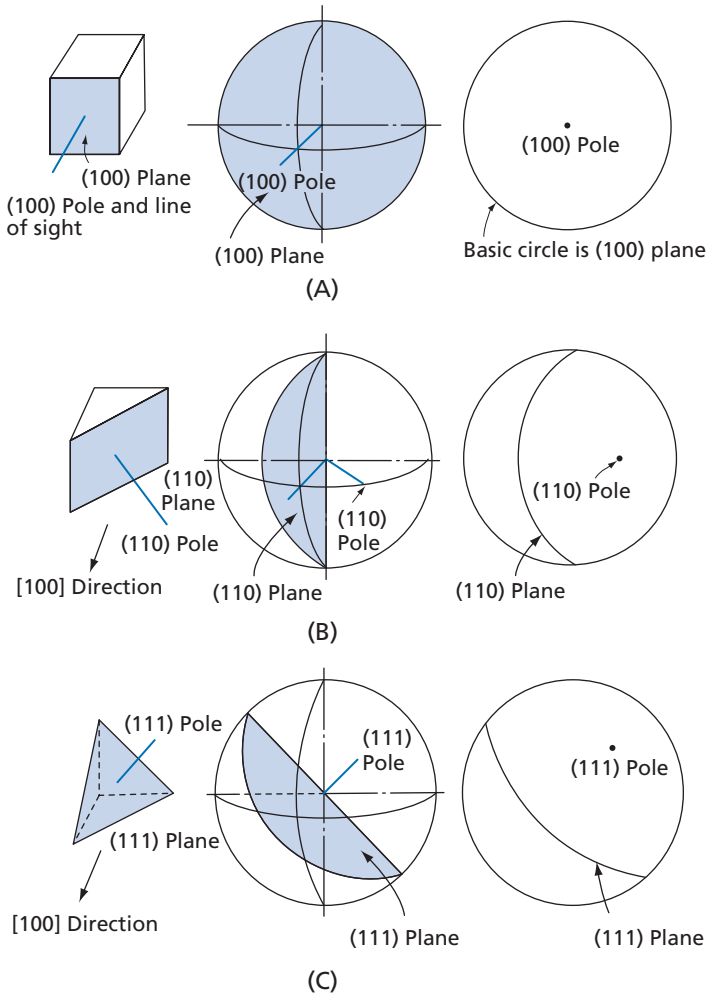

Fig. 1.20 Stereographic projections of several important planes of a cubic crystal. **(A)** The (100) plane, line of sight along the [100] direction. **(B)** The (110) plane, line of sight along the [100] direction. **(C)** The (111) plane, line of sight along the [100] direction

Many crystallographic problems can be solved by considering the stereographic projections of planes and directions in a single hemisphere, that is, normally the one in front of the plane of the paper. The three examples given in Fig. 1.20 have all been plotted in this manner. If the need arises, the stereographic projections in the rear hemisphere can also be plotted in the same diagram. However, it is necessary that the projections in the two hemispheres be distinguishable from each other. This may be accomplished if the stereographic projections of planes and directions in the forward hemisphere are drawn as solid lines and dots, respectively, while those in the rear hemisphere are plotted as dotted lines and circled dots, respectively. As an illustration, consider Fig. 1.21, in which the projections in both hemispheres of a single plane are shown. The (120) plane of a cubic lattice is used in this example.

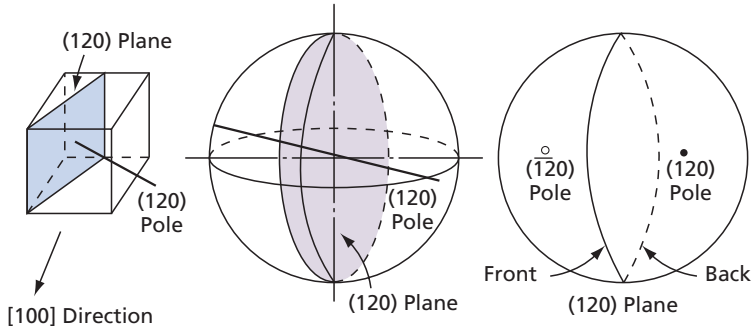

Fig. 1.21 Cubic system, the (120) plane, showing the stereographic projections from both hemispheres, line of sight the [100] direction

1.14 Directions that Lie in a Plane

Frequently one desires to show the positions of certain important crystallographic directions that lie in a particular plane of a crystal. Thus, in a body-centered cubic crystal one of the more important planes is {110}, and in each of these planes one finds two close-packed ⟨111⟩ directions. The two that lie in the (101) plane are shown in Fig. 1.22, where they appear as dots lying on the great circle representing the (101) plane.

1.15 Planes of a Zone

Those planes that mutually intersect along a common direction form the planes of a zone, and the line of intersection is called the *zone axis*. In this regard, consider the [111] direction as a zone axis. Figure 1.23 shows that there are three {110} planes that pass through the [111] direction. There are also three {112} planes and six {123} planes, as well as a number of higher indice planes that have the same zone axis. The pertinent {112} and {123} planes are shown in Fig. 1.24,

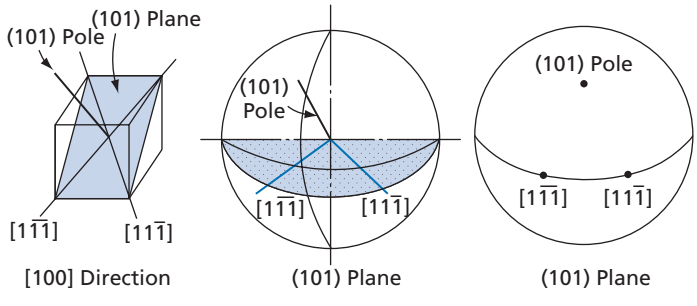

Fig. 1.22 Cubic system, the (101) plane and the two ⟨111⟩ directions that lie in this plane, line of sight [100]

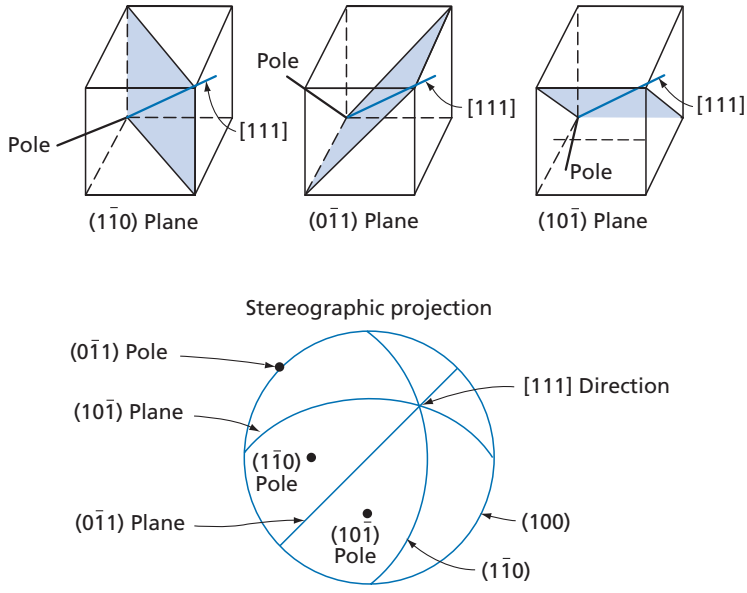

Fig. 1.23 Cubic system, zone of planes the zone axis of which is the [111] direction. The three {110} planes that belong to this zone are illustrated in the figures

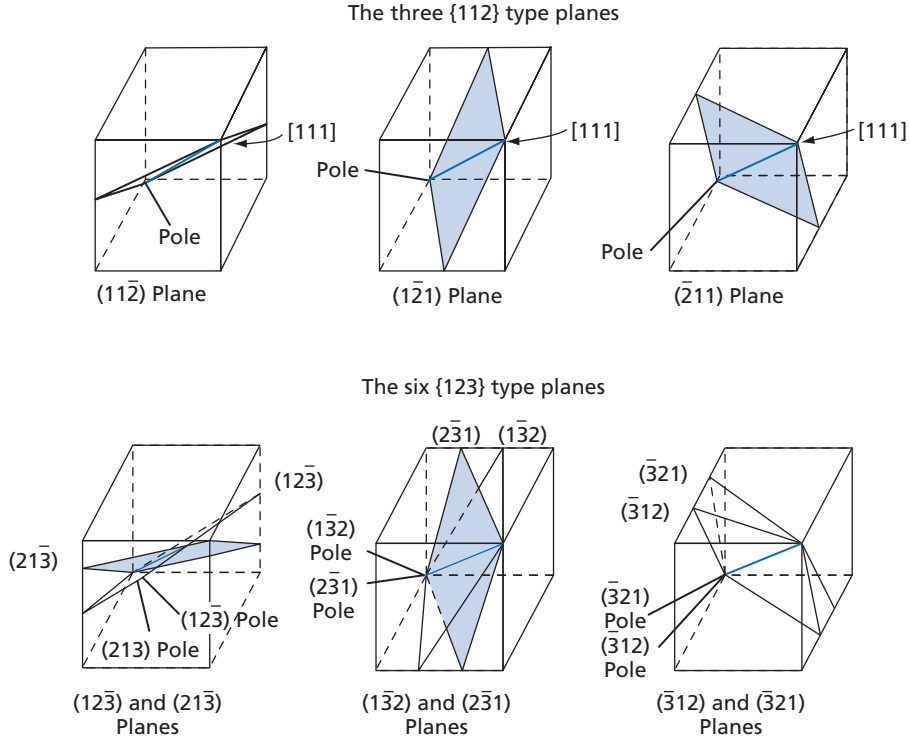

Fig. 1.24 The {112} and {123} planes that have [111] as their zone axis

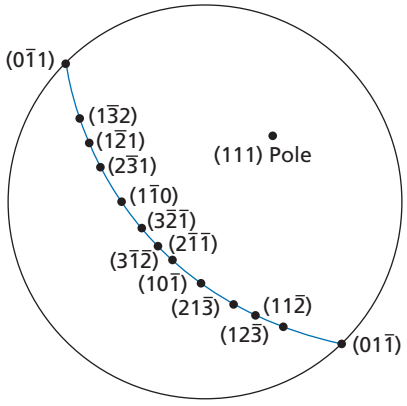

Fig. 1.25 Stereographic projection of the zone containing the 12 planes shown in Figs. 1.23 and 1.24. Only the poles of the planes are plotted. Notice that all of the planar poles lie in the (111) plane

whereas the stereographic projection of these and the previously mentioned {110} planes are shown in Fig. 1.25. Notice that in this latter figure only the poles of the planes are plotted, and it is significant that all of the poles fall on the great circle representing the stereographic projection of the (111) plane.

1.16 The Wulff Net

The *Wulff net* is a stereographic projection of latitude and longitude lines in which the north–south axis is parallel to the plane of the paper. The latitude and longitude lines of the Wulff net serve the same function as the corresponding lines on a geographical map or projection; that is, they make possible graphical measurements. However, in the stereographic projection we are primarily interested in measuring angles, whereas in the geographical sense distance is usually more important. A typical Wulff, or meridional, net drawn to 2° intervals is shown in Fig. 1.26.

Several facts about the Wulff net should be noted. First, all meridians (longitude lines), including the basic circle, are great circles. Second, the equator is a great circle. All other latitude lines are small circles. Third, angular distances between points representing directions in space can be measured on the Wulff net only if the points are made to coincide with a great circle of the net.

In the handling of many crystallographic problems, it is frequently necessary to rotate a stereographic projection corresponding to a given crystal orientation into a different orientation. This is done for a number of reasons. One of the most important is to bring experimentally measured data into a standard projection where the basic circle is a simple close-packed plane such as (100) or (111). Deformation markings, or other experimentally observed crystallographic phenomena, usually can be more readily interpreted when studied in terms of standard projections.

In solving problems with the aid of the Wulff net, it is customary to cover it with a piece of tracing paper. A common pin is then driven through the paper and into the exact center of the net. The paper, thus mounted, serves as a work sheet on which crystallographic data are plotted. The following two types of rotation of the plotted data are possible.

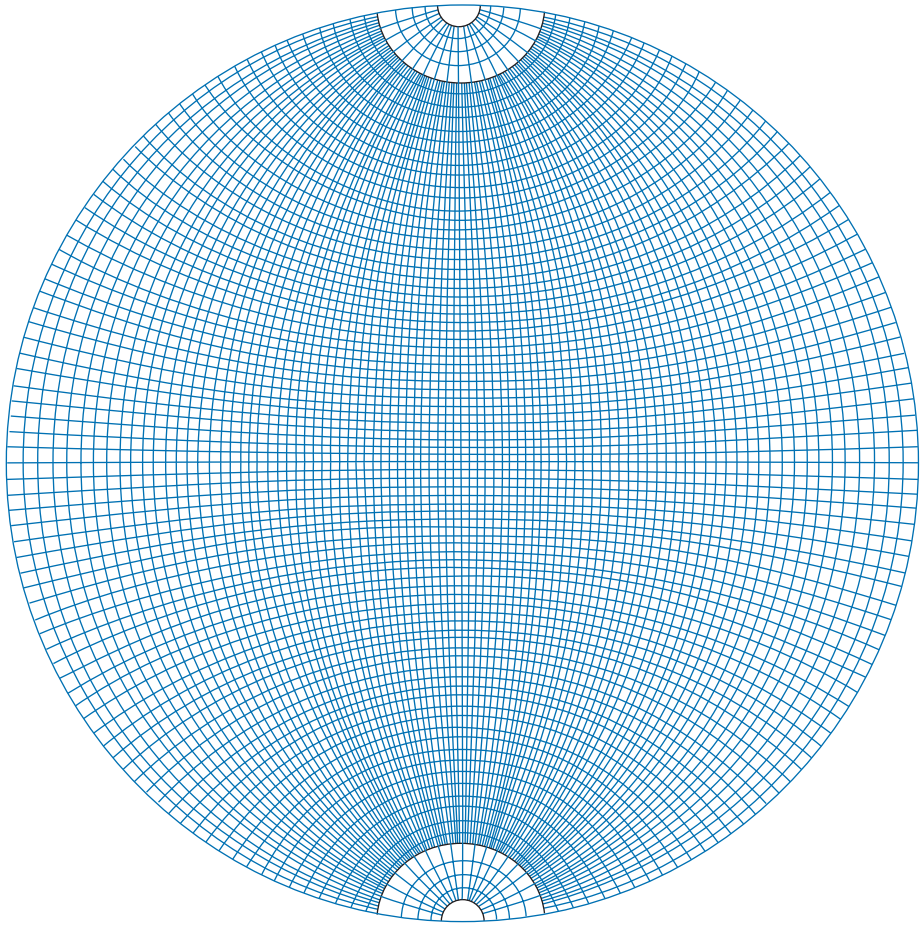

Fig. 1.26 Wulff, or meridional, stereographic net drawn with 2° intervals

Rotation About an Axis in the Line of Sight This rotation is easily performed by merely rotating the tracing paper, relative to the net, about the pin. As an example, let us rotate a cubic lattice 45° clockwise around the [100] direction as an axis. This rotation has the effect of placing the pole of the (111) plane, as plotted in Fig. 1.20C, on the equator of the Wulff net. Figure 1.27A shows the effect of the desired rotation on the orientation of the cubic unit cell when the cell is viewed along the [100] direction. Note that because the basic circle represents the (100) plane, a simple rotation of the paper by 45° about the pin produces the desired rotation in the stereographic projection.

Rotation About the North–South Axis of the Wulff Net This rotation is not as simple to perform as that given previously, which can be accomplished by merely rotating the work

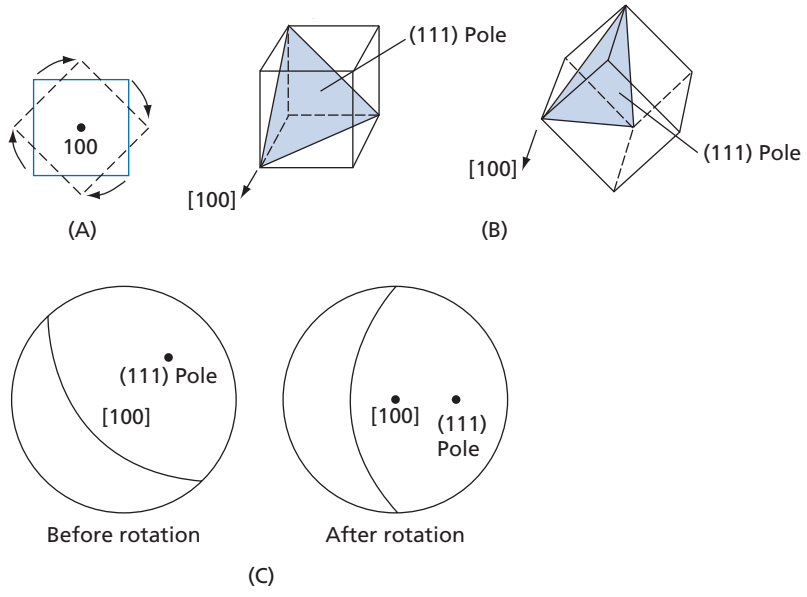

Fig. 1.27 Rotation about the center of the Wulff net. **(A)** The effect of the desired rotation on the cubic unit cell. Line of sight [100]. **(B)** Perspective view of the (111) plane before and after the rotation. **(C)** Stereographic projection of the (111) plane and its pole before and after rotation. Rotation clockwise 45° about the [100] direction

sheet about the pin. Rotations of this second type are accomplished by a graphical method. The data are first plotted stereographically and then rotated along latitude lines and replotted in such a manner that each point undergoes the same change in longitude. The method will be quite evident if one considers the drawings of Fig. 1.28. In the present example, it is assumed that the forward face (100) of

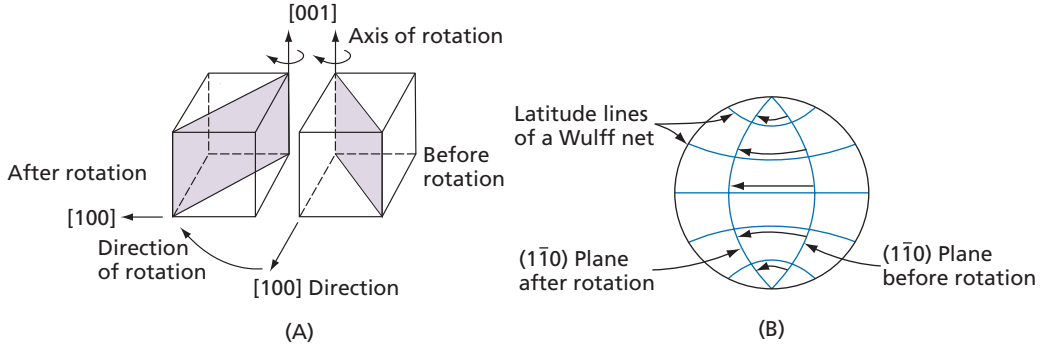

Fig. 1.28 Rotation about the north-south axis of the Wulff net. **(A)** Perspective views of the unit cell before and after the rotation showing the orientation of the (110) plane. **(B)** Stereographic projection showing the preceding rotation. For the sake of clarity of presentation, only the (1$\bar{1}$0) plane is shown. The rotation of the pole is not shown. Also, the meridians of the Wulff net are omitted

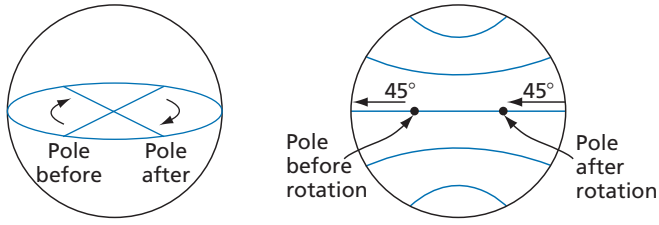

Fig. 1.29 The rotation of the pole of the $(1\bar{1}0)$ plane is given here. The diagram on the left shows the rotation in a perspective figure, whereas that on the right shows the motion of the pole along a latitude line of a stereographic projection which, in this case, is the equator

the unit cell is rotated to the left about the [001] direction as an axis. Consider now the effect of this rotation on the spatial orientation and stereographic projection of the $(1\bar{1}0)$ plane. In Fig. 1.28A, the right- and left-hand drawings represent the cubic unit cell before and after the rotation respectively. The effect of the rotation on the stereographic projection of the $(1\bar{1}0)$ plane is shown in Fig. 1.28B. Each of the curved arrows shown in this drawing represents a change in longitude of 90°. In these drawings, the pole of the $(1\bar{1}0)$ plane is not shown in order to simplify the presentation. The rotation that the (110) pole undergoes is shown, however, in Fig. 1.29.

By using simple examples, the two basic rotations that can be made when the Wulff net is used have been pointed out here. All possible rotations of a crystal in three dimensions can be duplicated by using these rotations on a stereographic projection.

1.17 Standard Projections

A stereographic projection, in which a prominent crystallographic direction or pole of an important plane lies at the center of the projection, is known as a standard stereographic projection. Such a projection for a cubic crystal is shown in Fig. 1.30, where the (100) pole is assumed to be normal to the plane of the paper. This figure is properly called a standard 100 projection of a cubic crystal. In this diagram, note that the poles of all the {100}, {110}, and {111} planes have been plotted at their proper orientations. Each of these basic crystallographic directions is represented by a characteristic symbol. For the {100} poles, this is a square, signifying that these poles correspond to four-fold symmetry axes. If the crystal is rotated 90° about any one of these directions, it will be returned to an orientation exactly equivalent to its original orientation. In a 360° rotation about a {100} pole, the crystal reproduces its original orientation four times. In the same fashion, a ⟨111⟩ direction corresponds to a three-fold symmetry axis, and these directions are indicated in the stereographic projection by triangles. Finally, the two-fold symmetry of the ⟨110⟩ directions is indicated by the use of small ellipses to designate their positions in the stereographic projection.

A more complete 100 standard projection of a cubic crystal is shown in Fig. 1.31. This includes the poles of other planes of somewhat higher Miller indices. Figure 1.31 can be considered to

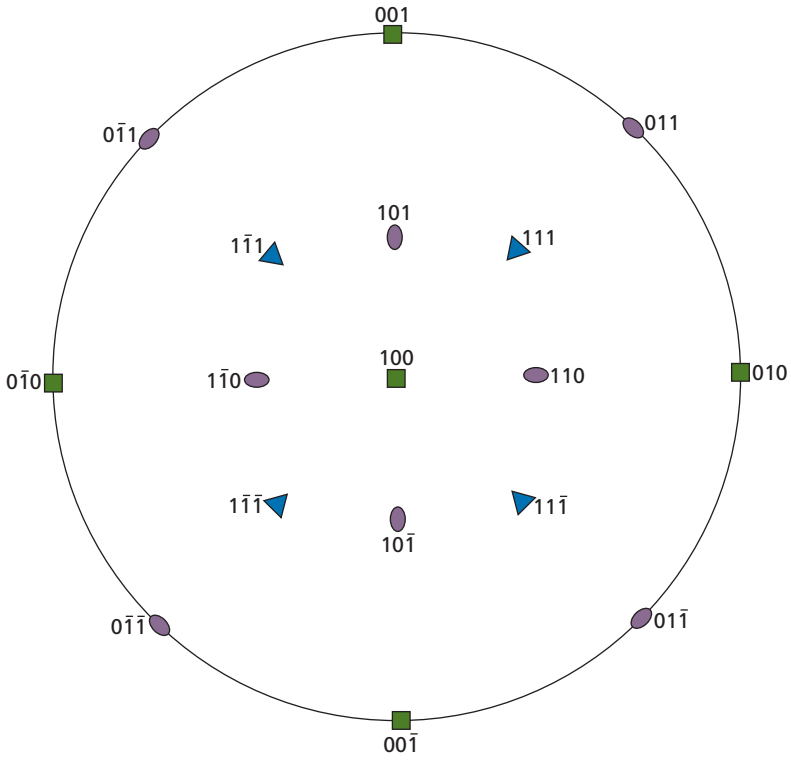

Fig. 1.30 A 100 standard stereographic projection of a cubic crystal

be either a projection showing the directions in a cubic crystal or the poles of its planes. This is because in a cubic crystal, a plane is always normal to the direction with the same Miller indices. In a hexagonal close-packed crystal, however, the projection showing the poles of the planes is not the same as one showing crystallographic directions.

Figure 1.32 shows a 111 standard projection that contains the same poles as the 100 projection in Fig. 1.31. The three-fold symmetry of the crystal structure about the pole of a {111} plane is clearly evident in this figure. At the same time, attention is called to the fact that the 100 projection of Fig. 1.31 also plainly reveals the four-fold symmetry about a {100} pole.

1.18 The Standard Stereographic Triangle for Cubic Crystals

The great circles corresponding to the {100} and {110} planes of a cubic crystal are also shown in the standard projections of Figs. 1.31 and 1.32. These great circles pass through all of the poles shown on the diagram except those of the {123} planes. At the same time, they divide the

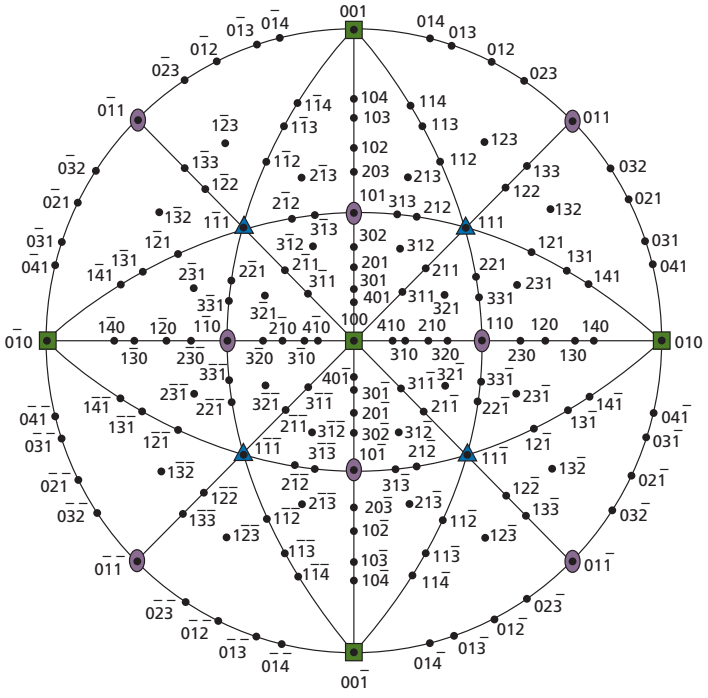

Fig. 1.31 A 100 standard stereographic projection of a cubic crystal showing additional poles

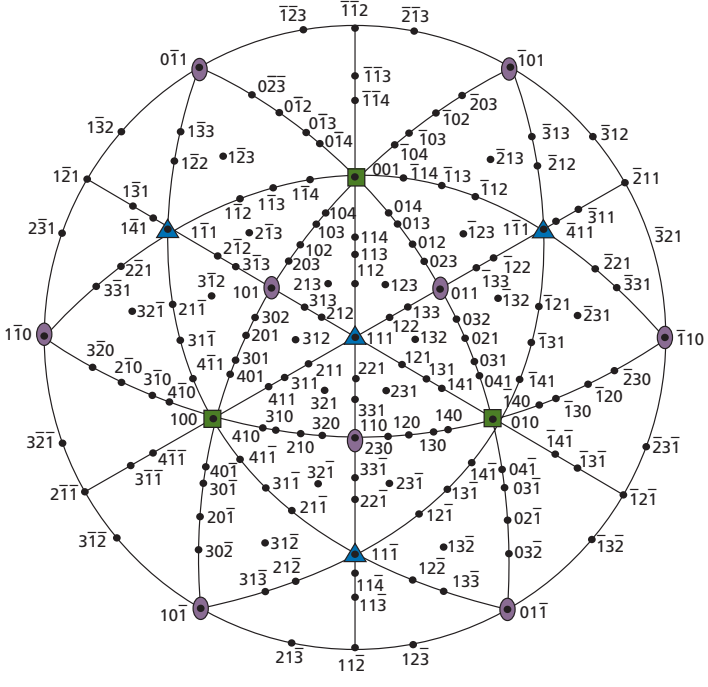

Fig. 1.32 A 111 standard projection of a cubic crystal

standard projection into 24 spherical triangles. These spherical triangles all lie in the forward hemisphere of the projection. There are, of course, 24 similar triangles in the rear hemisphere. An examination of the triangles outlined in Figs. 1.31 and 1.32 shows an interesting fact: in every case, the three corners of the triangles are formed by a ⟨111⟩ direction, a ⟨110⟩ direction, and a ⟨100⟩ direction. This is a highly significant observation, since it means that each triangle corresponds to a region of the crystal that is equivalent. In effect, this signifies that the three lattice directions, marked a_1, a_2, and a_3, and shown in Fig. 1.33, are crystallographically equivalent, because they are located at the same relative positions inside three stereographic triangles. To illustrate this point, let us assume that it is possible to cut three tensile specimens, with axes parallel to a_1, a_2, and a_3, out of a very large single crystal. If tensile tests were to be performed on these three smaller crystals now, one would expect to get identical stress-strain curves for the three specimens. A similar result should be obtained if some other physical property, such as the electrical resistivity, were to be measured along these three directions. The plotting of crystallographic data is often simplified because of the equivalence of the stereographic triangles. For example, if one has a large number of long, cylindrical crystals and wishes to plot the orientations of the individual crystal axes, this can be done conveniently in a single stereographic triangle, as shown in Fig. 1.34.

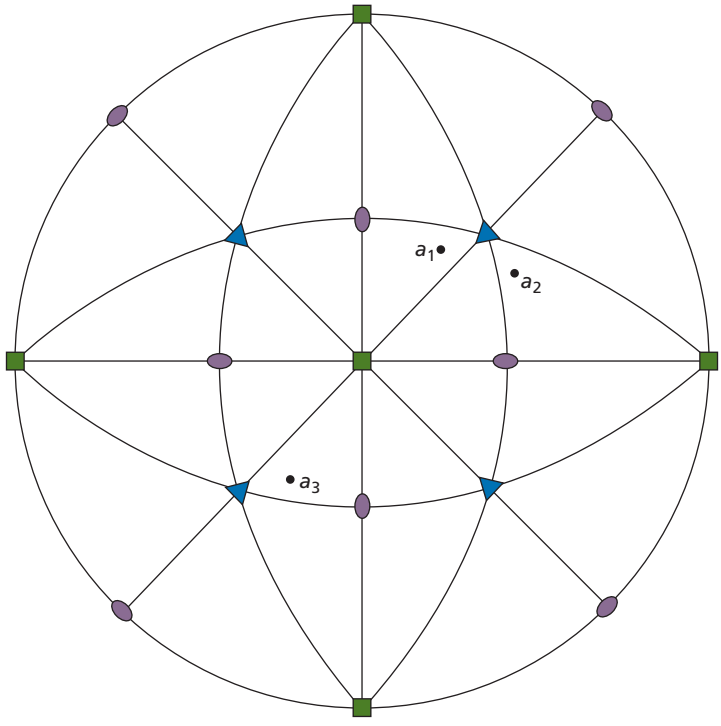

Fig. 1.33 The crystallographic directions a_1, a_2, and a_3 shown in this standard projection are equivalent because they lie in similar positions inside their respective standard stereographic triangles

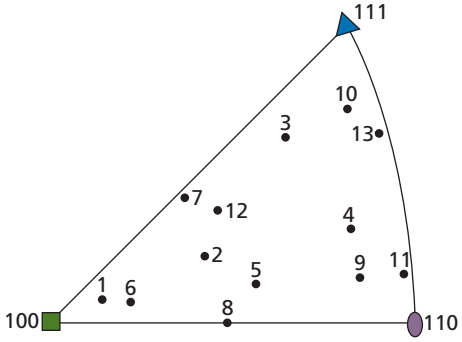

Fig. 1.34 When it is necessary to compare the orientations of a number of crystals, this often can be done conveniently by plotting the crystal axes in a single stereographic triangle, as indicated in this figure

Problems

1.1

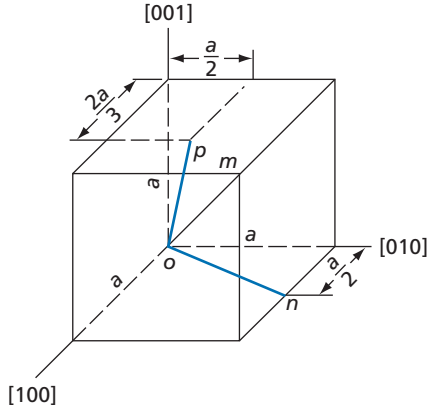

Determine the direction indices for (**a**) line *om*, (**b**) line *on*, and (**c**) line *op* in the accompanying drawing of a cubic unit cell.

1.2

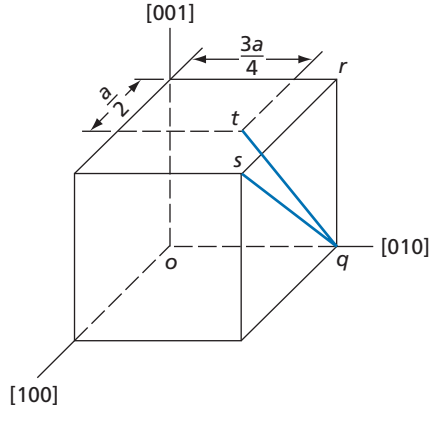

Determine direction indices for lines (**a**) *qr*, (**b**) *qs*, and (**c**) *qt*.

1.3

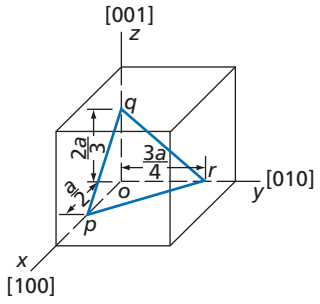

In this figure, plane *pqr* intercepts the *x*, *y*, and *z* axes as indicated. What are the Miller indices of this plane?

1.4

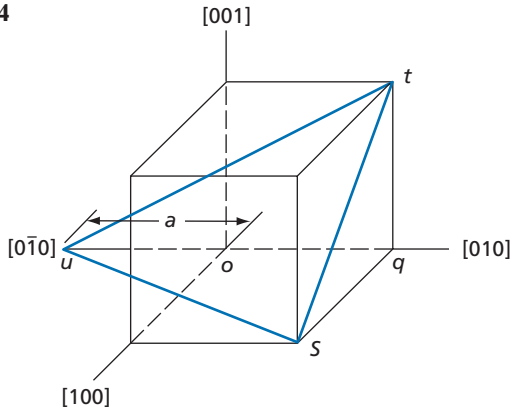

What are the Miller indices of plane *stu*?

1.5

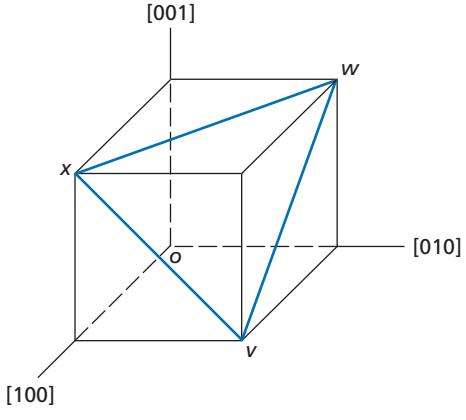

Write the Miller indices for plane *vwx*.

1.6 Linear density in a given crystallographic direction represents the fraction of a line length that is occupied by atoms whereas linear mass density is mass per unit length. Similarly, planar density is the fraction of a crystallographic plane occupied by atoms. The fraction of the volume occupied in a unit cell, on the other hand, is called the atomic packing factor. The latter should not be confused with bulk density, which represents weight per unit volume.

(a) Calculate the linear density in the [100], [110], and [111] directions in body-centered cubic (BCC) and face-centered cubic (FCC) structures.

(b) Calculate planar densities in (100) and (110) planes in bcc and fcc structures.

(c) Show that atomic packing factors for BCC, FCC, and hexagonal close-packed (HCP) structures are 0.68, 0.74, and 0.74, respectively.

1.7 Show that the c/a ratio (see Fig. 1.16) in an ideal hexagonal close-packed (HCP) structure is 1.63. (*Hint*: Consider an equilateral tetrahedron of four atoms which touch each other along the edges.)

1.8 Iron has a BCC structure at room temperature. When heated, it transforms from BCC to FCC at 1185 K. The atomic radii of iron atoms at this temperature are 0.126 and 0.129 nm for bcc and fcc, respectively. What is the percentage volume change upon transformation from BCC to FCC?

1.9

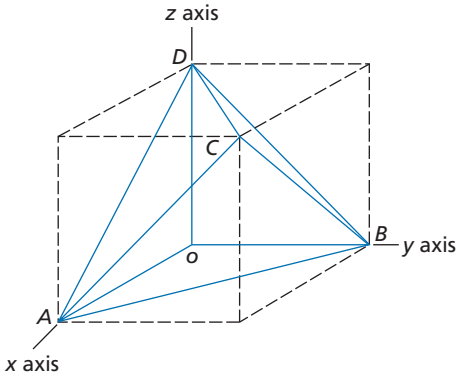

This diagram shows the Thompson Tetrahedron, which is a geometrical figure formed by the four cubic {111} planes. It has special significance with regard to plastic deformation in face-centered cubic metals. The corners of the tetrahedron are marked with the letters *A, B, C*, and *D*. The four surfaces of the tetrahedron are defined by the triangles *ABC, ABD, ACD*, and *BCD*. Assume that the cube in the above figure corresponds to a face-centered cubic unit cell and identify, with their proper Miller indices, the four surfaces of the tetrahedron.

1.10

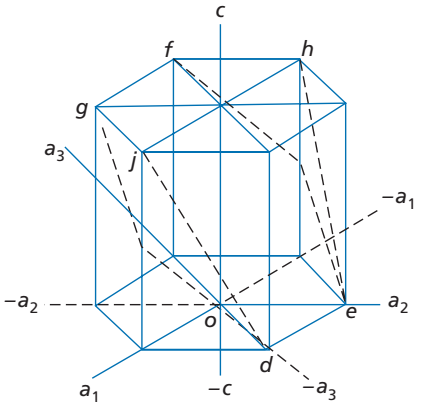

The figure accompanying this problem is normally used to represent the unit cell of a close-packed hexagonal metal. Determine Miller indices for the two planes, *defg* and *dehj*, that are outlined in this drawing.

1.11

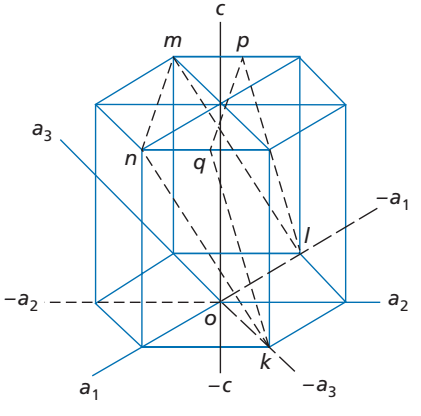

Two other hexagonal closed-packed planes, *klmn* and *klpq*, are indicated in this sketch. What are their Miller indices?

1.12

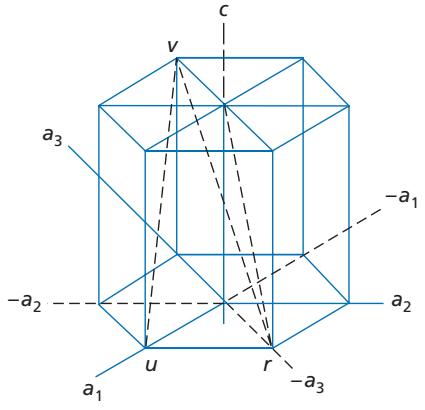

Determine the hexagonal close-packed lattice directions of the lines *rt, ut*, and *uv* in the figure for this problem. To do this, first determine the vector projection of a line in the basal plane and then add it to the *c* axis projection of the line. Note that the direction indices of the *c* axis are [0001], and that if [0001] is considered a vector its magnitude will equal the height of the unit cell. A unit distance along a digonal axis of Type I, such as the distance *or*, equals one-third of the length of $[2\bar{1}\bar{1}0]$ in Fig. 1.18. The magnitude of this unit distance is thus equal to $\frac{1}{3}[2\bar{1}\bar{1}0]$. Combine these two quantities to obtain the direction indices of each of the lines.

Stereographic Projection

The following problems involve the plotting of stereographic projections and require the use of the Wulff net, shown in Fig. 1.26, and a sheet of tracing paper. In each case, first place the tracing paper over the Wulff net and then pass a pin through the tracing paper and the center of the net so that the tracing paper may be rotated about the center of the net. Next, trace the outline of the basic circle on the tracing paper and place a small vertical mark at the top of this traced circle to serve as an index.

1.13 Place a piece of tracing paper over the Wulff net as described above, and draw an index mark on the tracing paper over the north pole of the Wulff net. Then draw on the tracing paper the proper symbols that identify the three ⟨100⟩ cube poles, the six ⟨110⟩ poles, and the four ⟨111⟩ octahedral poles as in Fig. 1.33. On the assumption that the basic circle is the (010) plane and that the north pole is [100], mark on tracing paper the correct Miller indices of all of the ⟨100⟩, ⟨110⟩, and ⟨111⟩ poles. Draw in the great circles corresponding to the planes of the plotted poles (see Fig. 1.33). Finally, identify these planes with their Miller Indices.

1.14 Place a piece of tracing paper over the Wulff net and draw on it the index mark at the north pole of the net as well as the basic circle. Mark on this tracing paper all of the poles shown in Fig. 1.30 in order to obtain a 100 standard projection. Now rotate this standard projection about the north–south polar axis by 45° so that the (110) pole moves to the center of the stereographic projection. In this rotation all of the other poles should also be moved through 45° along the small circles of the Wulff net on which they lie. This type of rotation is facilitated by placing a second sheet of tracing paper over the first and by plotting the rotated data on this sheet. This exercise shows one of the basic rotations that can be made with a stereographic projection. The other primary rotation involves a simple rotation of the tracing paper around the pin passing through the centers of both the tracing paper and the Wulff net.

References

1. "Metallography and Microstructures," *ASM Handbook*, Volume 9, ASM International, pp. 23–69.
2. K. Honda and S. Kaya, *Sci. Rep*. Tohoku Univ., 15, pp. 721–754 (1926).
3. S. Kaya, *Sci. Rep*. Tohoku Univ., 17, 639 (1928).
4. "Magnetic Anisotropy of Epitaxial Iron Films on Single-Crystal MgO.001. and Al2O3(112–0) Substrates," Yu. V. Goryunov and I. A. Garifullin, *Journal of Experimental and Theoretical Physics*, 88, 2 (1999), pp. 377–384.
5. A. R. Urade, I. Lahiri, and K. S. Suresh, *JOM* 75, 614–630 (2023).
6. *Smithells Metals Reference Book*, 6th Edition, edited by Eric A. Brandes, Butterworths, P 5.2.